Virologica Sinica 37 (2022) 591–600

Contents lists available at ScienceDirect

Virologica Sinica

journal homepage: www.keaipublishing.com/en/journals/virologica-sinica
www.virosin.org

Research Article

Phospho-proteomics identifies a critical role of ATF2 in pseudorabies virus replication

Fang-Fang Jiang [a,1], Ren-Qi Wang [a,1], Chao-Yue Guo [a], Ke Zheng [a], Hai-Long Liu [b], Le Su [a], Sheng-Song Xie [b], Huan-Chun Chen [a], Zheng-Fei Liu [a,*]

[a] State Key Laboratory of Agricultural Microbiology, Hongshan Laboratory and Key laboratory of Preventive Veterinary Medicine in Hubei Province, College of Veterinary Medicine, Huazhong Agricultural University, Wuhan, 430070, China
[b] Key Lab of Agricultural Animal Genetics, Breeding, and Reproduction of Ministry of Education, Huazhong Agricultural University, Wuhan, 430070, China

ARTICLE INFO

Keywords:
Pseudorabies virus (PRV)
Transcription activator factor-2 (ATF2)
iTRAQ
Proteomics
Phosphorylation

ABSTRACT

Pseudorabies virus (PRV), an etiological agent of pseudorabies in livestock, has negatively affected the porcine industry all over the world. Epithelial cells are reported as the first site of PRV infection. However, the role of host proteins and its related signaling pathways in PRV replication is largely unclear. In this study, we performed a quantitative phosphoproteomics screening on PRV-infected porcine kidney (PK-15) epithelial cells. Totally 5723 phosphopeptides, corresponding to 2180 proteins, were obtained, and the phosphorylated states of 810 proteins were significantly different in PRV-infected cells compared with mock-infected cells ($P < 0.05$). GO and KEGG analysis revealed that these differentially expressed phosphorylated proteins were predominantly related to RNA transport and MAPK signaling pathways. Further functional studies of *NF-κB, transcription activator factor-2* (*ATF2*), *MAX* and *SOS* genes in MAPK signaling pathway were analyzed using RNA interference (RNAi) knockdown. It showed that only ATF2-knockdown reduces both PRV titer and viral genome copy number. JNK pathway inhibition and CRISPR/Cas9 gene knockout showed that ATF2 was required for the effective replication of PRV, especially during the biogenesis of viral genome DNA. Subsequently, by overexpression of the *ATF2* gene and point mutation of the amino acid positions 69/71 of ATF2, it was further demonstrated that the phosphorylation of ATF2 promoted PRV replication. These findings suggest that ATF2 may provide potential therapeutic target for inhibiting PRV infection.

1. Introduction

Pseudorabies virus (PRV), an etiological agent for Aujeszky's disease, is a swine pathogen of the *Alphaherpesvirinae* subfamily which is associated with some devastating neurological and respiratory disorders in piglets or abortion in pregnant sows (Mettenleiter, 2000). The geographical widespread of pseudorabies caused by PRV has resulted in huge economic losses in the porcine industry, although in recent decades, several countries have been declared PRV-free in domestic pig populations (Moynagh, 1997; Pensaert and Morrison, 2000). The establishment of lifelong latency in peripheral ganglia is the hallmark of PRV and other alpha herpesviruses infections, resulting in the extremely difficult eradication of PRV between domestic pigs and wild boar. The most effective method for achieving a PRV-free pig herd is vaccination (Freuling et al., 2017). Unexpectedly, in 2011, a new PRV variant emerged in some pig farms in China where the Bartha-K61 vaccine was used (An et al., 2013; Yu et al., 2014). This means that there is the need to develop new prevention and treatment strategies to deal with future PRV mutations.

Effective prevention and treatment strategies rely on a complete understanding of PRV pathogenesis. As a strict intracellular parasitic pathogen, the replication cycle of PRV depends on host cells. The understanding of interactions between virus and host, and the identification of the indispensable host genes for virus proliferation are crucial for the development of novel vaccines and the exploration of potential therapeutic targets (Li et al., 2017). However, the interactions between PRV and host cellular factors are not well known. Host-pathogen interactions are complex and dynamic, and represent an area of focused research (Söderholm et al., 2016). There is increasing evidence showing that hijacking host post-translational mechanisms including protein

* Corresponding author.
E-mail address: lzf6789@mail.hzau.edu.cn (Z.-F. Liu).
[1] Fang-Fang Jiang and Ren-Qi Wang contributed equally to this work.

https://doi.org/10.1016/j.virs.2022.06.003
Received 22 July 2021; Accepted 2 June 2022
Available online 7 June 2022

phosphorylation is a vital strategy for viruses to effectively utilize host signal transduction (Wojcechowskyj et al., 2013; Ravikumar et al., 2015). High-throughput phosphoproteomics based on mass spectrometry is a powerful tool for analyzing the changes in host protein phosphorylation during virus infections (Macek et al., 2009). The proteomics data analysis of PRV infection on PK-15 cells has been reported (Flori et al., 2008; Wu et al., 2012). They found that many biological processes were altered during PRV infection and PRV infected epithelial cell line generates a diverse set of host miRNAs and a special cluster of viral miRNAs, which might facilitate PRV replication in cells. However, there are still few research reports on the high-throughput data analysis of PRV-dependent host protein phosphorylation transduction pathway (Yin et al., 2021).

Activating transcription factor 2 (ATF2) is a member of the activating protein 1 (AP1) family. In addition to being involved in gene regulation as a transcription factor, ATF2 also plays a role in the control of DNA damage response and the activity of the heteromeric amino acid transporters (HATs) complex (Bhoumik and Ronai, 2008). ATF2 also has a nuclear localization signal, which plays an important role in transporting extracellular stimulus signals to the nucleus (Yuan et al., 2009). Its activation is mediated by the phosphorylation of the threonine 69/71, which is activated by stress-activated protein kinases (SAPKs), p38, JNK and other kinases. Studies have shown that after PRV infection of PK-15 cells, the expression level of ATF2 does not change significantly, but its phosphorylation level is significantly increased (Yeh et al., 2008). However, whether the phosphorylation level of ATF2 has an effect on PRV infection has not been reported yet.

Here, we performed isobaric tags for relative and absolute quantitation (iTRAQ) and LC-MS/MS quantitative phosphoproteomics on PRV-infected PK-15 cells, which identified 5,723 phospho-peptides, corresponding to 2,180 proteins, including 810 proteins showing significant changes in phosphorylation level during early PRV infection. Kyoto Encyclopedia of Genes and Genomes (KEGG) differential enrichment analysis showed that PRV infection influences the MAPK signaling pathway, including several kinases and cellular factors. Functional studies showed that ATF2 is required for efficient PRV replication, and is activated by PRV through the c-Jun N-terminal kinase (JNK) signaling pathway. Epigenetic expression of the ATF2 wildtype and mutants at 69/71 phosphorylation sites further demonstrated that the increased phosphorylation level of ATF2 promotes PRV replication.

2. Materials and methods

2.1. Cell culture and virus propagation

PK-15 cells (ATCC CCL-33) and Madin-Darby bovine kidney (MDBK) cells (ATCC CCL-22) were purchased from the China Center for Type Culture Collection, the Cas9 stable-expressed PK-15 cell line (Cas9 PK-15) was a gift from Professor Shuhong Zhao (Key Lab of Agricultural Animal Genetics, Breeding, and Reproduction of Ministry of Education, Huazhong Agricultural University). These cell lines were cultured and maintained in Dulbecco's modified Eagle's medium (DMEM; Invitrogen) supplemented with 10% (v/v) FBS (Gibco, catalog no.10099-141), 100 U/mL of penicillin and 10 μg/mL streptomycin sulfates with 5% CO_2 at 37 °C. The FBS level in the medium was reduced to 2% during virus infection. Wild-type PRV (WT-PRV) was isolated from an aborted pig fetus, and was propagated in PK-15 cells as described previously (Wu et al., 2012).

2.2. Virus infection and sample preparation for phosphoproteome analysis

PK-15 cells were grown to 80% confluence in 175 cm^2 flasks (or 6-well plates, it depends on the specific experimental requirements), then the medium was discarded and cells were washed three times with ice-cold serum-free DMEM. Cells were precooled in 4 °C for 30 min, and infected with WT-PRV at a multiplicity of infection (MOI) of 10. Residual input viruses were then removed at 1.5 h post-attachment at 4 °C. Cells were washed three times with ice-cold serum-free DMEM and resuspended in fresh medium before further incubation in 5% CO_2 at 37 °C for 2.5 h. Mock infected cells were treated with 0.5% DMEM instead of PRV infection using the same procedures. After 2.5 h post infection (hpi) (The time to collect the virus depends on the specific experiment), the medium was discarded and cells were washed three times with ice-cold PBS before lysing of cells in SDT lysis buffer [4% (w/v) SDS, 100 mmol/L Tris/HCl, 1 mmol/L DTT, pH 7.6]. Lysis samples were boiled for 15 min followed by ultrasonic processing (work 10 s, interval 15 s, 10 cycles). The supernatant was centrifuged at 13,200 ×*g* for 30 min, and then quantified with the BAC Protein Assay Kit (Bio-Rad, USA). Protein quality was confirmed with SDS-PAGE (Schagger, 2006). Each group of samples was labeled with an equivalent amount of peptide (200 g) according to the iTRAQ reagent-8 plex Multiplex Kit (AB SCIEX) instructions.

The mixed phosphopeptides were enriched using Titanium dioxide (TiO_2). The solution was vacuum-freeze-dried and diluted with 1 × DHB buffer [3% 2,5-dihydroxybenzoic acid (DHB), 80% acetonitrile (CAN), 0.1% Trifluoroacetate (TFA)]. TiO_2 beads were added into the solution and oscillated for 40 min. The solution was then centrifuged and the supernatant was discarded. Retained beads were washed three times with washing buffer 1 (30% CAN, 1%TFA) followed by washing buffer 2 (80% CAN, 0.1% TFA) three times. The phosphorylated peptides were eluted with elution buffer, vacuumized, and dissolved in 30 μL 0.1% FA (Formic acid) and then 20 μL was taken for liquid chromatography tandem mass spectrometry (LC-MS/MS) analysis (Larsen et al., 2005). The mass spectrometer was operated in positive ion mode. MS data was acquired using a data-dependent top 10 method dynamically choosing the most abundant precursor ions from the survey scan (300–1800 *m/z*) for high energy collision dissociation (HCD) fragmentation. Automatic gain control (AGC) target was set to 3e6, and maximum inject time to 10 ms. Dynamic exclusion duration was 40.0 s. Survey scans were acquired at a resolution of 70,000 at m/z 200 and resolution for HCD spectra was set to 17,500 at *m/z* 200, and isolation width was 2 *m/z*. Normalized collision energy was 30 eV and the underfill ratio, which specifies the minimum percentage of the target value likely to be reached at maximum fill time, was defined as 0.1%. The instrument was run with peptide recognition mode enabled.

2.3. Mass spectrometry and data processing

The phosphopeptides were separated using a high-performance liquid chromatography (HPLC) liquid phase system Easy nLC1000 (flow rate, nL), and the samples were injected three times. Buffer solutions were as follows: buffer A, 0.1% formic acid aqueous solution; buffer B, 0.1% formic acid acetonitrile aqueous solution (84% acetonitrile). The column was balanced at 95% buffer A. The samples were added to a C18 chromatographic column by an automatic sampler [100 μm (diameter) × 2 cm (length), 5 μm (particle size)] and separated by a C18 analytical column (75 μm × 250 mm, 3 μm) at a flow rate of 250 nL/min. The gradient of the related liquid phase was as follows: 0–220 min, buffer B ranged linearly from 0% to 55%; 220–228 min, buffer B ranged linearly from 55% to 100%; 228–240 min, buffer B was maintained at 100%.

The samples were separated by capillary HPLC and analyzed by Q-Exactive mass spectrometer (Thermo Finnigan). Analysis was performed using the following settings: analysis time, 240 min; detection method, positive ion; parent ion scanning range, 350–1800 *m/z*; first-level mass spectral resolution, 70,000 at *m/z*200; AGC target, 3e6; first-level maximum Ion Trap (IT), 20 ms; number of scan ranges, 1; dynamic

exclusion, 30 s. Mass charge ratios of peptides and peptide fragments were collected by the following methods: 10 fragments (MS2 scan) after each full scan; MS2 activation type, HCD; isolation window, 2 *m/z*; secondary-mass spectral resolution, 17,500 at *m/z* 200; microscans, 1; secondary-level maximum IT, 60 ms; normalized collision energy, 29 eV; underfill ratio, 0.1%.

The MS data were saved as raw files, then identified and quantitatively analyzed by Mascot v2.2 and Proteome Discoverer 1.4 (Thermo Scientific) software. The database used in this study was UniProt_Sus_scrofa_35472_20161104.fasta (35,472 sequences were included and the download date was 2016-11-04). When checking the library, the the raw files were submitted to the Mascot server through Proteome Discoverer, and then the database was searchable (Beausoleil et al., 2006; Olsen et al., 2006).

2.4. Western blot analysis

Cell pellets were washed for three times with ice-cold PBS, and were lysed in 1 × SDS-PAGE loading buffer [250 mmol/L Tris-HCL, 10% (w/v) SDS, 0.5% (w/v) bromophenol blue, 50% (v/v) glycerin, and 5% (v/v) 2-mercapto-ethanol] supplemented with a protease inhibitor cocktail (Catalog no. P8340, Sigma-Aldrich) and a phosphatase inhibitor cocktail (Catalog no. ZD416-1, Zomanbio) on ice for 5 min. Samples were then denatured at 100 °C for 10 min, and the subsequent steps were performed as described previously (Wang et al. 2017; Wang et al. 2018). The primary antibodies used in this study included anti-MAX (Catalog no. ab72997, Abcam; 1:2,000); anti-SOS1 (Catalog no. GTX133774, GeneTex; 1:1,000); anti-NF-κB (Catalog no. E381, Abcam; 1:2000); anti-RSK2 (Catalog no. NBP1-19295, Novus; 1:500); anti-phospho-RSK1/RSK2 (Catalog no. AF892, Biorbyt; 1:2,000); anti-ATF2 (Catalog no. SC242, Santa Cruz; 1:1,000); anti-phospho-ATF2 (Catalog no. 9221, GST; 1:1, 000); anti-MAPK (Erk 1/2) (Catalog no. 9102, GST; 1:1,000); anti-GAPDH (Catalog no. 60004-1-lg, Proteintech; 1:5,000); anti-FLAG (Catalog no. AE005, Abcam; 1:10,000). To confirm equal sample loading the membranes were stripped and labeled with anti-GAPDH.

2.5. ATF2 transfection and RNA interference

ATF2 transfection was conducted following Lipofectamine 2000 (Invitrogen). The suspended PK-15 cells (ATF2-knockout), which were transfected with EGFP-tag recombinant plasmid (pcDNA3.1-EGFP, constructed and preserved by our laboratory), were detected by flow cytometry. Fluorescence of transfected PK-15 cells (ATF2-knockout) was analyzed by CytExport 2.0 CellQuest Pro software. The small interfering RNA (siRNA) used in this study (including the nonspecific control siRNA) were purchased from Gene Pharm (http://www.genepharma.com/productslist.), and three siRNA peer genes were designed and the most optimal one was chosen (Supplementary Table S1). siRNA was used at a concentration of 50 nmol/L.

2.6. Measurement of plaque formation unit (PFU) for viral titers

After PK-15 cells were grown in T-175 flasks until about 90% confluence, an MOI of 0.1 of PRV was added. At about 72 h post infection, cells were harvested and put into the refrigerator at −80 °C, and freeze-thawed for twice. After MDBK cells were grown in 24-well plates until about 60% confluence, the virus was sequentially diluted with DMEM containing 2% FBS, 100 U/mL of penicillin and 10 μg/mL streptomycin, and 200 μL per well of the 10^{-5}, 10^{-6} and 10^{-7} dilutions were added in triplicate to 24-well plates, followed by gentle shaking. Plates were incubated at 37 °C and 5% CO_2 for 2 h. During this period, the plates were shaked horizontally for 3–5 times every 15 min. The wells were then covered with 1 mL DMEM containing 4% sodium carboxymethyl cellulose, 2% FBS, 100 U/mL penicillin and 10 μg/mL streptomycin sulfate and incubated at 37 °C with 5% CO_2 for 48 h. Cells were fixed with 10% neutral formaldehyde overnight at room temperature, washed with flowing water, and treated with 0.2 mL crystal violet dye solution. Plates were incubated at room temperature of 37 °C for 20 min, following which the crystal violet dye solution was discarded, and plates were washed and plaques were counted using a Stereo-Microscope.

2.7. RNA extraction and quantitative real-time reverse transcription (qRT-PCR)

Total RNA was extracted from treated cells with TRIzol® reagent (Invitrogen) following the manufacturer's instructions. One microgram of total RNA was reversely transcribed to complementary DNA (cDNA) with Easy-Script One-Step gDNA Removal and cDNA Synthesis Super-Mix (TRAN, cat. L21011), the reaction system is prepared as follows: Total RNA (DNA free) 50 ng–5 μg; Primer (10 μmol/L) 1 μL; EasyScript®RT/RI Enzyme Mix 1 μL; 2 × ES Resction Mix 10 μL; gDNA Remover 1 μL; RNase-free Water up to 20 μL, following which 1 μL cDNA was used in a SYBR Green real-time PCR system (Applied Biosystems, USA). qRT-PCR analysis was performed using Quantstudio™ Real-Time PCR Software (ViiA™-7 System, Life Technologies). Each sample was assayed three times and the data were normalized to porcine glyceraldehye-3-phosphate dehydrogenase (GAPDH) mRNA.

2.8. Inhibitor treatment and MTT cytotoxicity assay

PK-15 cells were treated with 20 μmol/L SP600125 inhibitor (Selleck, cat. S1460S) and 20 μmol/L SB202190 inhibitor (Selleck, cat. S1077), which were dissolved in DMSO. Cells were exposed to the inhibitors for 4 h and then infected with PRV at an MOI of 0.05. The negative control cells were treated with an equal volume of DMSO. Inhibitor cytotoxicity was detected by MTT assay (Mosmann, 1983). Cells were treated with different concentrations of pharmacological compounds for 24 h, then formazan was added to the cells for 2 h, followed by addition of isopropanol and finally, absorbance was detected with a PerkinElmer Multimode Plate Reader EnVision.

2.9. Plasmid construction

The lentivirus packaging plasmids, pMD2.G and pSPAX2 were purchased from Addgene (Watertown, MA), and the single guide (sg) RNA expression plasmid plenti-sgRNA-GFP was a gift from Professor Xingxu Huang (School of Life Science and Technology, Shanghai Tech University). Plasmid pcDNA3.1 (+) (catalog no. V709-20) was purchased from TaKaRa (Dalian, China). sgRNAs were designed to target the *ATF2* gene by using 20-bp guide sequences immediately followed by a protospacer adjacent motif (PAM) sequence. The 20-bp guide sequences were analyzed according to the *ATF2* gene with the help of the bioinformatics tool sgRNACas9 (Xie et al., 2014). The GC content of the guide sequences was set within 40%–60%. To construct the sgRNA expression vectors targeting *ATF2*, we synthesized primers followed by annealing with a PCR machine, then cloned the annealed product into the plenti-sgRNA-GFP vector. To construct the plasmid pATF2 and pmATF2 (T69A, T71A), we amplified the ATF2 coding regions from cDNA derived from PK-15 cells by PCR and the purified product was used as a template to amplify the mutant fragment by point mutation (T69A, T71A), then fragments were cloned into pcDNA3.1 to yield pATF2, pmATF2 (T69A, T71A), respectively. The primer sequences are described in Supplementary Table S2. The plasmid pFLAG was used as a negative control.

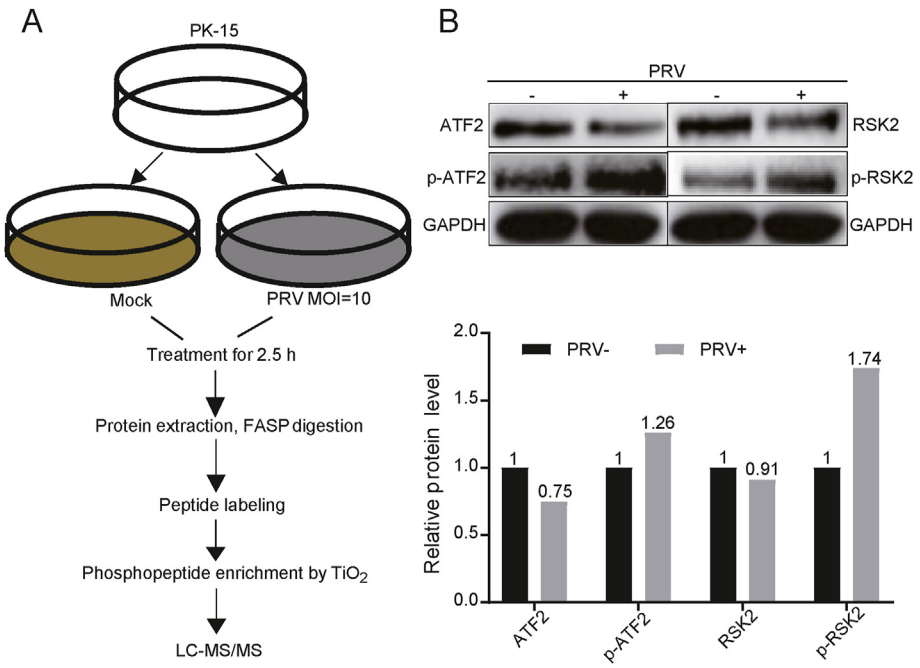

Fig. 1. Phosphoproteomic profiling of pseudorabies virus (PRV)-infected PK-15 cells by iTRAQ/LC-MS/MS. The omics experiment was divided into two groups, each with three biological replications. The mock group, also comprising PK-15 cells, was used as a negative control and treated in the same manner as the PRV-infection group. **A** Workflow for the phosphoproteomics experiment in PRV-infected PK-15 cells. **B** Confirmation of differentially expressed proteins and phosphoproteins of ATF2/RSK2 by Western blot. Total protein was extracted and electrophoresed by SDS-PAGE. ATF2, phospho-ATF2, RSK2 and phospho-RSK2 antibodies were used to detect the expression of ATF2 and RSK2, respectively. Protein levels were normalized to GAPDH.

2.10. Construction of gene knockout cell lines

Through the third-generation lentivirus packaging system (pMD2. G: pSPAX2: plenti-sgRNA-GFP = 1:2:3), we obtained an sgRNA (GTGAGTTGTTTCTACAACAGAGG) lentivirus that expressed the target *ATF2* gene sequence in HEK293T cells, then Cas9 stable expressing PK-15 cell line was infected with lentivirus. Positive clonal cells (ATF2 knock-out PK-15 cells) were screened by limited dilution with fluorescence, and whether the cells expressed the *ATF2* gene was determined by Sanger sequencing and Western blotting.

2.11. Restoration of ATF2 expression in knockout cell lines

Transfection was conducted using Lipofectamine 2000 (Invitrogen). The plasmid pATF2 was transfected into ATF2-knockout cell line and the restored expression of ATF2 was detected by Western blotting.

2.12. Statistical analysis

The statistical analyses of data were performed with GraphPad Software using two-way ANOVA, followed by Duncan's multiple range test (DMRT) to evaluate the significant differences, the significance level is indicated as $^{***}P < 0.001$, $^{**}P < 0.01$, $^{*}P < 0.05$; $P > 0.05$ not significant (n.s.).

3. Results

3.1. Phosphoproteomic profiling of PRV-infected PK-15 cells by iTRAQ/LC-MS/MS

Recently, proteomic study of PRV infection of PK-15 cells was reported (Yang et al., 2017), however, global signaling pathways and host factors involved in PRV replication have not been well elucidated. To analyze the changes of early PRV infection on the phosphorylation of host proteins, 2.5 hpi was selected as the sample collection time point, (Flori et al., 2008; Tombacz et al., 2011). Additionally, cells were infected with PRV, an MOI of 10 as previously described (Yan et al., 2019). To quantify relative fold changes in host protein phosphorylation of PK-15 cells by PRV infection, we used TiO_2-enriched phosphopeptide technology combined with iTRAQ technology and LC-MS/MS-based phosphoproteome analysis, coupled with bioinformatics analysis and functional assays. The workflow of phosphoproteomic profiling was described in Fig. 1A.

In total, 5723 phosphopeptides originating from 2180 proteins were identified. Among the 2180 proteins, 810 of these proteins was significantly expressed ($P < 0.05$). There were 678 phosphopeptides with phosphorylation level increased by 1.2-fold, corresponding to 484 proteins, and 603 phosphopeptides with phosphorylation level decreased by 0.83-fold, corresponding to 446 proteins in the PRV-infected group compared with the control group according to the FC > 1.2 (Fold change), $P < 0.05$ (Supplementary Tables S3, S4, S5).

To further confirm the phosphoproteomics data, we used phospho-specific antibodies to validate the iTRAQ phosphorylation protein ratios. Based on a previous study of PRV-induced upregulation of ATF2 (Yeh et al., 2008), we chose ATF2 (pT69 and pT71) and another ribosomal kinase RSK2 (pS378) from the phosphoproteomics panel. Immunoblot results showed that the ATF2 and RSK2 phosphorylation levels were enhanced upon the addition of PRV for 2.5 h (Fig. 1B), which was consistent with the phosphoproteomics results.

A recent study showed that very short incubations with low concentrations of adenosine diphosphate (ADP) in cell lysate triggers a sustained stimulation of intracellular signaling cascades using phosphoproteomics (Beck et al., 2017). To rule out the potential influence of the lysate, a control experiment with virus-free lysates was carried out. The result showed that equal amount of ATF2 appeared in PRV stock (containing

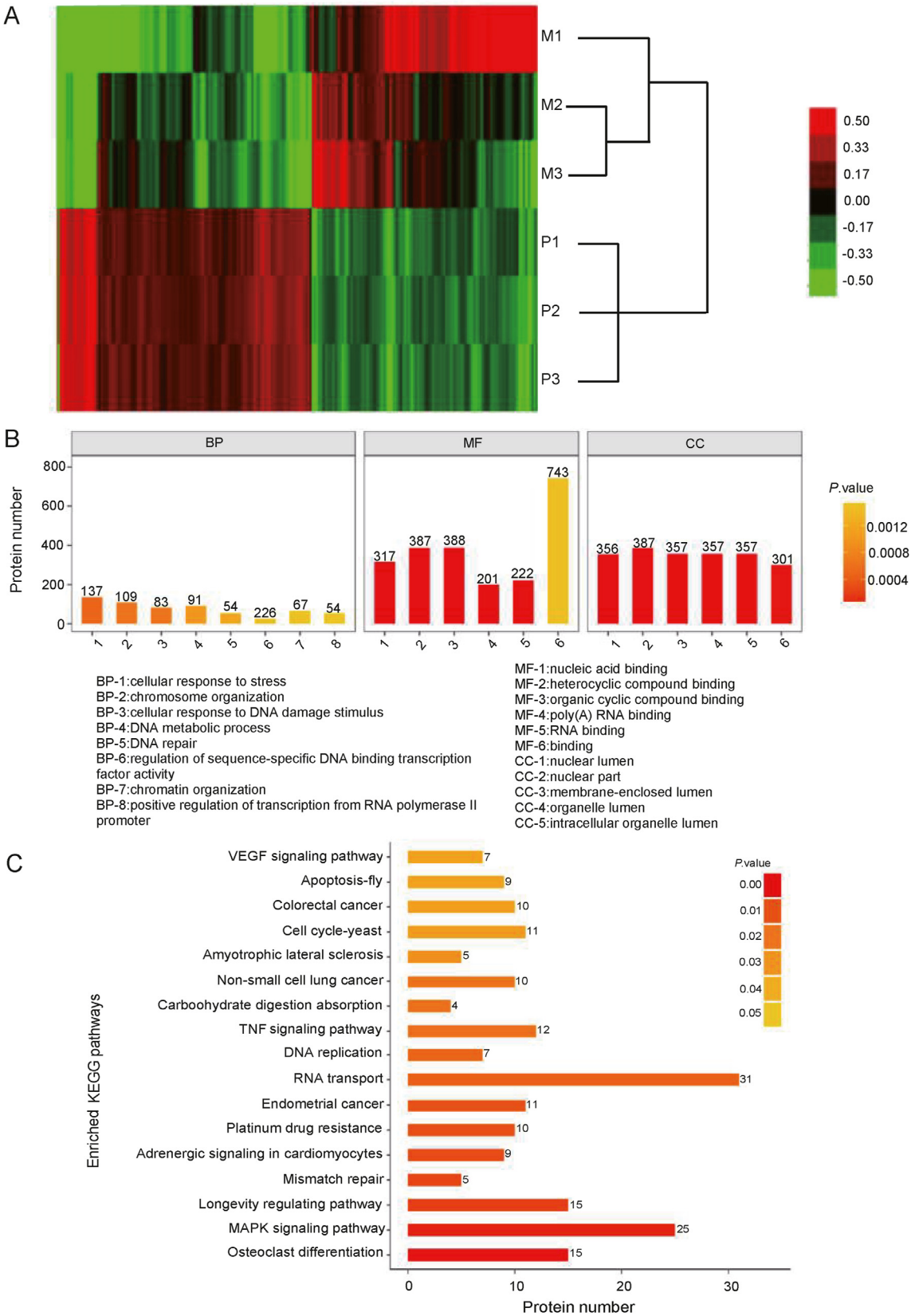

Fig. 2. Bioinformatic analysis of differentially phosphorylated proteins. **A** Clustering of phosphoproteomics data. M1, M2 and M3 represent three biological replicates of the mock infected group; P1, P2 and P3 represent three biological replicates of the PRV infected group. **B** Enriched GO terms analysis of the differentially phosphorylated proteins. The top 20 phosphorylated proteins were divided in three ontologies. (biological processes (BP), molecular functions (MF), cellular components (CC)). **C** Statistics for significantly enriched pathways during PRV infection with KEGG analysis. Statistical significance (*P* value) differentially expressed proteins was calculated with Fisher's Exact Test.

PRV and cell lysates), mock (DMEM) and normal PK-15 cell lysates; phosphorylated ATF2 was more abundant in PRV infected PK-15 cells compared with mock (DMEM) and normal PK-15 cell lysates, while there is almost no difference between mock (DMEM) and normal PK-15 cell lysates (Supplementary Fig. S1). The result suggests that PRV infection induces up regulation of ATF2 phosphorylation.

3.2. Functional enrichment analysis of phosphorylated proteins differentially expressed upon PRV infection

The protein relative expression data was used for hierarchical clustering analysis (Fig. 2A). In the result of clustering grouping, the similarity of data patterns within groups is higher, while the similarity of data patterns between groups is lower, indicating that the rationale and accuracy of the selected differential proteins were reliable.

To further explore the impact of 810 differentially expressed proteins in cell physiological process and discover internal relations between these proteins, enrichment analysis was performed. We annotated the differentially expressed proteins, into three ontologies (biological processes, molecular functions, cellular components) with the Gene Ontology (GO) and UniProt databases (Ashburner et al., 2000) (Supplementary Table S6, S7, S8, S9), and the enriched GO Terms are shown (Fig. 2B, Supplementary Table S10). Among the three gene ontologies, the frequency of each GO term appears almost at the same level, but the proportion of binding in the molecular function is significantly higher than that of other terms in the same group.

To understand the enrichment of differentially expressed host proteins in the signaling pathways post PRV infection, we analyzed the data using the KEGG pathway database (Kanehisa and Goto, 2000). The statistical analysis of significant enrichment KEGG pathway revealed multiple pathways are regulated to some extent by PRV infection but the MAPK signaling pathway contained the most significant and enriched differentially expressed proteins (Fig. 2B and C, Supplementary Table S11, S12, S13). These results showed that the MAPK pathway is significantly stimulated after PRV infection.

3.3. RNAi-mediated knockdown of PRV-responsive phosphoproteins in the MAPK signaling pathway

To address whether PRV-responsive phosphoproteins in the MAPK pathway are important for PRV replication, we selected *NF-κB, ATF2, MAX* and *SOS* genes which are located in the different sub-pathways of the greater MAPK signaling pathway and have been observed to undergo changes in phosphorylation level following PRV infection according to the MAPK pathway map (Map04010 by CytoScape software (Version number: 3.2.1), Supplementary Table S11). We designed siRNAs to target the four host genes (three siRNAs per gene), and measured the siRNA efficiency at the mRNA and protein levels using RT-qPCR and Western blot, respectively, showing that these siRNAs can silence target gene sequences (Fig. 3A and B).

To further confirm the effect of these genes, PK-15 cells were transfected with effective siRNAs against *NF-κB, ATF2, MAX* and *SOS* genes and infected with WT-PRV at an MOI of 0.05 at 12 h post-transfection. At 12 hpi, we monitored PRV titer by plaque assay and viral genome copy number by RT-qPCR (Fig. 3C and D). The results showed that, ATF2-knockdown reduces both PRV titer ($P < 0.001$) and viral genome copy number ($P < 0.05$), while NF-κB-knockdown only reduces viral genome copy number ($P < 0.05$), MAX-knockdown and SOS-knockdown only reduce PRV titer (MAX: $P < 0.01$, SOS: $P < 0.05$). These results suggest that ATF2-knockdown inhibits virus replication.

3.4. Effect of inhibitor-mediated interference of ATF2 gene signal transduction on PRV replication

ATF2 is a member of the ATF-CREB family of transcription factors, which are involved in cellular responses to stress (Hai et al., 1989; van Dam et al., 1995). Previous studies have indicated that phosphorylation of ATF2 is triggered by stress-activated protein kinases p38 (Gueorguiev et al., 2006), JNK (Gupta et al., 1995), protein kinase C (PKC) (Lim et al., 2005), or phosphatidyl inositol 3 kinase (PI3K) (Recio and Merlino, 2002). To investigate whether p38 or JNK cellular pathway activates ATF2 phosphorylation following PRV infection (Map04010, Supplementary Table S11), we selected inhibitors that specifically targeted the two signaling pathways: SP600125-JNK (Shen et al., 2017) and SB202190-p38 (Duzgun et al., 2017). Firstly, we detected the cytotoxicity of the different inhibitors by MTT assay. The results indicated that PK-15 cell growth rate was more than 85% for both inhibitors at concentrations lower than 40 μmol/L (Fig. 4A). Then, to determine the optimal concentration of inhibitors, PK-15 cells treated with two inhibitors at different concentrations were infected with WT-PRV and then, phosphorylation of ATF2 was detected at 2.5 hpi by Western blot. The results showed that both inhibitors can inhibit ATF2 phosphorylation and 20 μmol/L was the optimal concentration for inhibition (Fig. 4B).

To determine which pathways (JNK or p38) contribute to PRV replication, we infected cells with WT-PRV and detected viral titers in inhibitor-treated or untreated cells at 0, 3 and 12 hpi by plaque assay. The results showed that PRV titers were significantly reduced when the

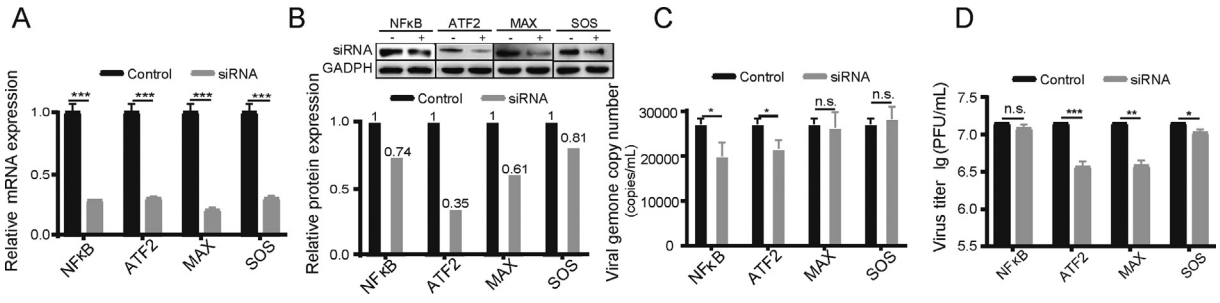

Fig. 3. siRNA-mediated knockdown of PRV-responsive phosphoproteins in the MAPK signaling pathway. **A** PK-15 cells were transfected with specific siRNAs against NF-κB, ATF2, MAX, and SOS, and gene transcription was detected by real-time PCR. Individual gene expression was normalized to a non targeted control siRNA (negative control). **B** Cell lysate was loaded onto 1 × SDS-PAGE gel and the interference efficiency of siRNA was analyzed by Western blot. Negative control siRNA was set as the loading control (100%). The normalized relative protein amount was quantified by densitometry scanning (ImageJ2x) and GAPDH was used as the internal control. **C** The effect of siRNA on PRV titer was quantified by plaque assay. **D** The effect of siRNA on PRV genome copy number was quantified by qRT-PCR. $^{*}P < 0.05$; $^{**}P < 0.01$; $^{***}P < 0.001$; n.s., not significant.

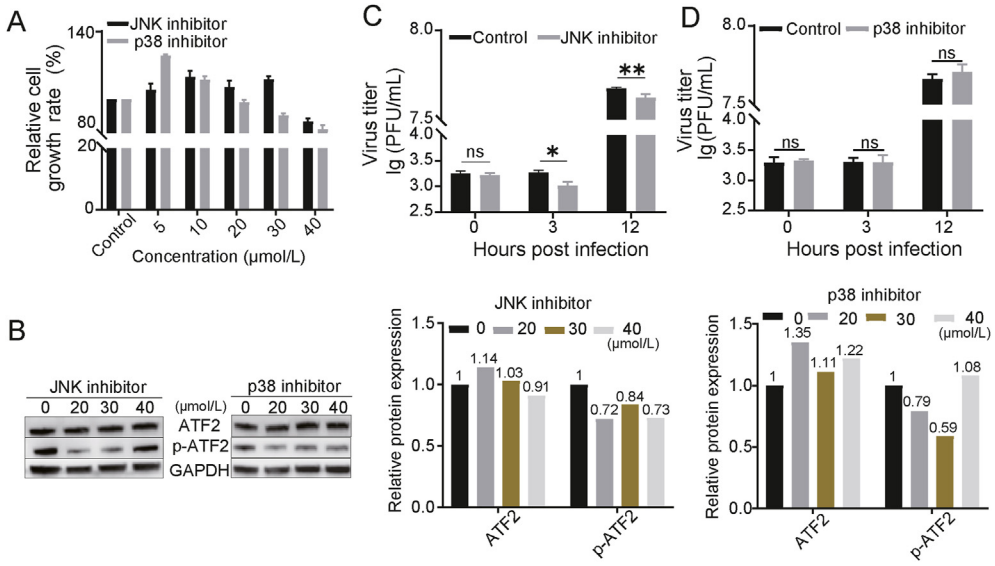

Fig. 4. Inhibitor-mediated interference of ATF2 gene signal transduction on PRV replication. **A** Cytotoxicity of JNK (SP600125) and p38 (SB202190) inhibitors in PK-15 cells was analyzed by MTT assay. **B** Effect of JNK (SP600125) and p38 (SB202190) inhibitors on ATF2 phosphorylation. PK-15 cells were treated with 0.1% DMSO or increasing amounts (20, 30, 40 μmol/L) of SP600125 and SB202190. After incubation for 4 h, all cells were infected with PRV at an MOI of 10. Phosphorylation of ATF2 was analyzed by Western blot at 2.5 hpi. PRV replication titer was quantified by plaque assay in the presence of SP600125 (**C**) and SB202190 (**D**), respectively. The concentrations of SP600125 and SB202190 were both 20 μmol/L. $*P < 0.05$; $**P < 0.01$; $***P < 0.001$; n.s., not significant.

JNK signaling pathway was blocked, while inhibition of the p38 signaling pathway had no significant effect on virus proliferation (Fig. 4C and D). These data indicate that the JNK pathway regulates ATF2 phosphorylation and PRV replication.

3.5. Knockout of ATF2 gene inhibits PRV replication in PK-15 cells

To further explore the role of the *ATF2* gene in virus proliferation, the ATF2 knock-out PK-15 cells were constructed by CRISPR/Cas9 lentivirus (Fig. 5A). Subsequently, Sanger sequencing and Western blot showed that ATF2-KO-#1 and ATF2-KO-#4 did not express ATF2 protein at all (Fig. 5B and C). The transfection efficiency of PK-15 was measured with Flow Cytometry. The results showed that about 48.4% of PK-15 cells expressed fluorescent EGFP plasmid (Supplementary Fig. S2). Then the pATF2 plasmid was transfected into cells, and the expression level of ATF2 was restored to some extent in ATF2-KO-#1 and ATF2-KO-#4 (Fig. 5C).

We used WT-PRV at an MOI of 0.05 to infect ATF2-KO-#1, ATF2-KO-#4 cells and control cells. Furthermore, ATF2-KO-#1 and ATF2-KO-#4 cells respectively transfected with pATF2 plasmid before WT-PRV infection. Then PRV titers were monitored at 0, 3 and 12 hpi by plaque assay. The results showed that PRV proliferation was suppressed in ATF2 knock-out cells at the middle and late infection time points, and ATF2 plasmid transfection could restore PRV production (Fig. 5D).

3.6. Phosphorylation of ATF2 promotes PRV replication

Furthermore, to investigate whether the effect of ATF2 on PRV replication through translational or post-translational phosphorylation, we overexpressed complete ATF2 and 69/71 (T69A, T71A) mutated ATF2 into PK-15 cells. The results showed that the phosphorylation level of wildtype ATF2 protein was increased, but the phosphorylated mutated ATF2 (T69A, T71A) was decreased (Fig. 6A).

Then effects of ATF2 mutation on PRV replication were compared. Complete ATF2 or 69/71 (T69A, T71A) mutated ATF2 was transfected into PK-15 cells, followed by WT-PRV infection at 24 h post-transfection, and virus titer was measured by PFU assay at 0 and 12 hpi. The results showed that transfection of complete ATF2 significantly increased the viral titers of PRV at 12 hpi, while mutated ATF2 (T69A, T71A) had no significantly reduced effect on the viral titers compared with the control group (Fig. 6B). These data suggest that expression of ATF2 increases PRV replication and the phosphorylation level of ATF2 plays a positive role in PRV growth.

4. Discussion

PRV is an important veterinary virus that causes huge economic losses in livestock. PK-15 cells are an appropriate model for the study of the interactions between virus and host (Wu et al., 2012; Liu et al., 2016; Yang et al., 2017). Recent report documented the proteomic profile of PK-15 cells during PRV infection (Yang et al., 2017). In our study, we applied the isobaric tags for relative and absolute quantification (iTRAQ) labeling coupled with liquid chromatography-tandem mass spectrometry in PRV-infected PK15 cells, and identified 4333 proteins. About 466 proteins were expressed differently, including 234 up-expressed proteins and 232 down-expressed proteins. We found significant differences in phosphorylated state of about 810 proteins. Two types (phosphorylated and unphosphorylated) of representative proteins were verified by Western blotting. According to the results of GO Analysis, the differentially expressed proteins were assigned to the groups of biological process, molecular function or cellular components. The analysis of pathway (KEGG) indicated that there was an enhanced activation of the MAPK signaling pathway in PK-15 cells during PRV infection, including the variation of 25 proteins in phosphorylation level, which is in accordance with the previous report (Yang et al., 2017). Coincidentally, some reports showed that the viral infections may be bounded to the MAPK pathways, such as Japanese

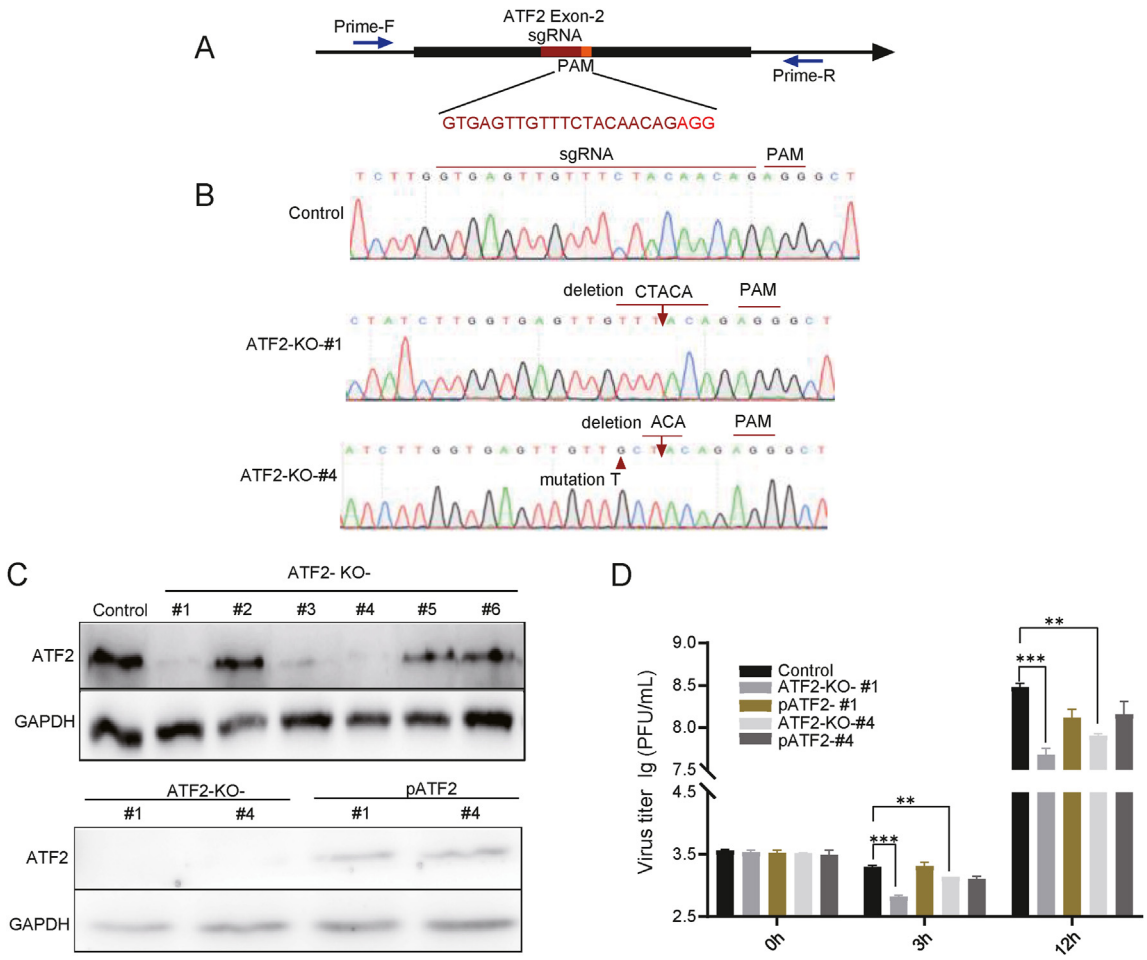

Fig. 5. PRV replication was inhibited by *ATF2* gene knockout in PK-15 cells. **A** Schematic diagram of the generation of ATF2-null Cas9 PK-15 cells. sgRNA (GTGAGTTGTTTCTACAACAGAGG) was designed against exon 2 of ATF2. Prime-F (ACCCCAACACCAACACGATT) and Prime-R (TCTCCCCAATAATTTTTCTGTGTCT) were used to amplify the ATF2-exon sequence to detect the correct knockout. **B** Sequencing peak diagram of control and ATF2-KO-#1 and ATF2-KO-#4 Cas9-expressing PK-15 cells. **C** Verification of ATF2-null and ATF2-supplemented expression in ATF2-KO-#1 and ATF2-KO-#4. Cas9-expressing PK-15 by Western blot. Total protein was extracted and electrophoresed by SDS-PAGE. ATF2 antibody was used to detect the expression of ATF2. **D** The effect of *ATF2* gene on PRV replication in PK-15 cells. ATF2-KO-#1 and ATF2-KO-#4 cells were directly infected with PRV or transfected with pATF2 plasmid and then infected with PRV, and viral titers were detected by plaque assay at 0, 3 and 12 hpi. $^{**}P < 0.01$; $^{***}P < 0.001$.

encephalitis virus (Xing et al., 2021), enterovirus (Zhu et al., 2020), coxsackievirus B3 (He et al., 2019), Human immunodeficiency virus type 1 (Kumar et al., 1998), HSV-1 (McLean and Bachenheimer, 1999; Zachos et al., 1999), and human cytomegalovirus (Rodems and Spector, 1998). A recent study showed that PRV triggers proteasomal degradation of the Janus kinases Jak 1 to inhibit both type I and type III IFN-induced STAT1 phosphorylation, suppressing IFN-induced ISGs expression (Yin et al., 2021). However, the phosphorylation level of the MAPK signaling pathway affects the life cycle of PRV remains unclear.

ATF2, an activating transcription factor, is a member of the activator protein 1 (AP1) family. ATF2 forms homologous or heterologous dimers with other AP1 family members (CREB, Fos, Maf and Jun etc.), and regulates gene expression in the nucleus (Yuan et al., 2009; Inoue et al., 2018; Ma et al., 2018). Our results indicated that the interference of *ATF2* gene effectively inhibit the replication of virus. We also found that the overexpression of ATF2 facilitated PRV proliferation, which was consistent with the findings of Yeh et al. (Yeh et al., 2008). These results suggested that ATF2 participates in the replication process of PRV.

The phosphoproteomic data indicated that PRV infection upregulated the phosphorylation level of ATF2 in the PK-15 cells. And the mutation of ATF2 phosphorylation reduced PRV titer.

Previous studies showed that the transcriptional activation of ATF2 is mediated by p38 and JNK (Gupta et al., 1995; Ouwens et al., 2002; Wang et al., 2011). We found that the inhibition of JNK signal transduction decreased ATF2 phosphorylated level. These results indicated that the proliferation of PRV depends on the activation of the ATF2, which was mediated by JNK. Previous report demonstrated inhibition of JNK and p38 reduced cell apoptosis during PRV infection (Yeh et al., 2008). The inhibition of c-Jun N-terminal kinase induces the blocking of ATF2 phosphorylation and reduces ganglion cell death. However, in our study there were no dramatically effects while inhibiting the activity of p38. These results indicated that the p38 plays almost no effects on the phosphorylated ATF2 level.

The establishment of lifelong latent infection in the peripheral nervous system is a distinct character of alpha-herpesvirus, which restricts the treatment of viral infection diseases. The latency-associated transcript (LAT) was expressed to inhibit neuronal apoptosis, and promotes

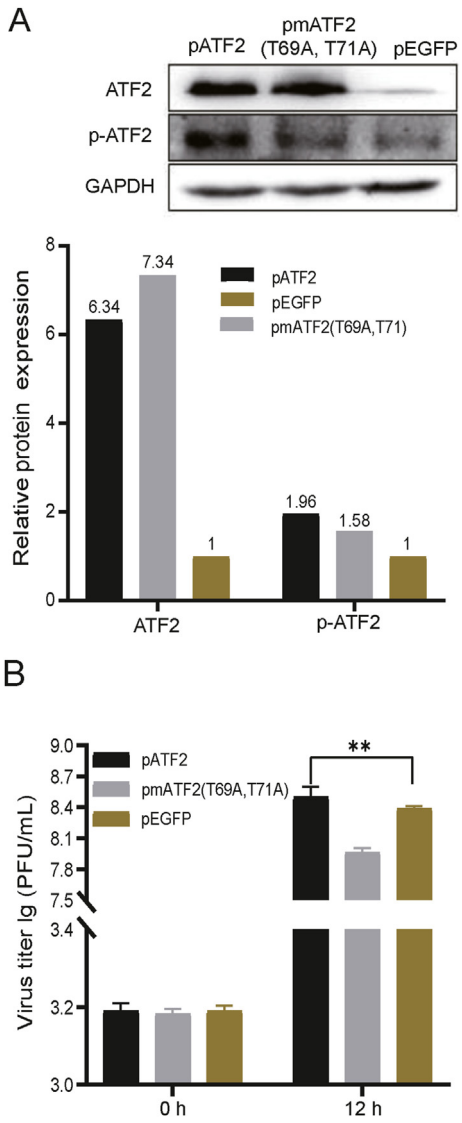

Fig. 6. Phosphorylation and activation of ATF2 promote PRV proliferation. **A** Western blot analysis to detect the expression of complete or mutant ATF2 (T69A and T71A) in PK-15 cells. Plasmids pEGFP, pATF2, or pmATF2 (T69A and T71A) were transfected into PK-15 cells for 24 h. Total protein was extracted from cell lysate and electrophoresed by SDS-PAGE. Antibodies of ATF2 and phospho-ATF2 were used to detect the expression of ATF2 and phosphorylated ATF2. p-ATF2 represents phosphorylated ATF2. **B** PK-15 cells were tansfected with complete ATF2 or mutant ATF2 (T69A and T71A) gene for 24 h, EGFP plasmid was used as a negative control, and then the cells were infected by PRV at an MOI of 1. Virus titers were determined at 0 and 12 hpi. $^{**}P < 0.01$.

the establishment of latent infection (Stevens et al., 1987). The hypokalemia-induced neuronal apoptosis induced the upregulation of phosphorylation and the transcriptional activity of ATF2 was enhanced (Yuan et al., 2009). The inhibition of ATF2 facilitated neurons avoiding from cell apoptosis, and formation of heterodimers between ATF2 and *c*-Jun promoted neuronal apoptosis. Furthermore, ATF2 is involved in the maintenance of nerve-injury mediated tactile pain and hyperthermalgesia (Salinas-Abarca et al., 2018). The transcription and phosphorylation levels of ATF2 are also associated with the replication of multiple viruses, including Epstein-Barr virus (EBV), HCMV and Kaposi's sarcoma-associated herpesvirus (Sharma-Walia et al., 2005; Yuan et al., 2009; Murata et al., 2011). Together, there might be a correlation between the ATF2 and neuron survival, which stimulates reactivation of PRV from latent infection.

5. Conclusions

In summary, our study revealed the interaction between the phosphorylation level of the host protein ATF2 and the proliferation of PRV: PRV can activate ATF2 through JNK Pathway, the proliferation of PRV depends on the phosphorylation activation of ATF2 protein, up-regulation of the phosphorylation level of ATF2 will promote PRV replication. It will be important to extend this study to the field of antiviral drug research and development, as the findings presented here suggest that ATF2 may provide potential new therapeutic targets for inhibiting PRV infection.

Data availability

The mass spectrometry proteomics data was deposited to the ProteomeXchange Consortium via the PRIDE partner repository with the dataset identifier PXD014685. MS data in PRIDE is available online (URL: https://www.ebi.ac.uk/pride/archive/projects/PXD014685/priva).

Ethics statement

The study was reviewed and approved by Research Ethics Committee of the College of Veterinary Medicine, Huazhong Agricultural University, Hubei, Wuhan, China.

Author contribution

Fang-Fang Jiang: conceptualization, methodology, investigation, data curation, formal analysis, visualization, writing-original draft. Ren-Qi Wang: methodology, investigation, formal analysis, data curation. Chao-Yue Guo: writing-review & editing. Ke Zheng: conceptualization, methodology. Hai-Long Liu: formal analysis, visualization. Le Su: resources, investigation. Sheng-Song Xie: resources. Huan-Chun Chen: supervision. Zheng-Fei Liu: conceptualization, methodology, project administration, writing-review & editing, funding acquisition.

Conflict of interest

The authors declared that no competing interest exists.

Acknowledgments

This work was supported by the Natural Science Foundation of China (32170155, 31770191) and the Major Science and Technology Projects of Hubei Province (2021ABA005) to Z.F.L.

We thank Shuhong Zhao for the generous gift of the Cas9 stable-expressing PK-15 cell line, and Xing-Xu Huang for the kind gift of the plenti-sgRNA-GFP plasmid. We also thank Songsong Zou for his guidance and help with the writing of the article. We obtained data analysis support from China National GenBank.

Appendix A. Supplementary data

Supplementary data to this article can be found online at https://doi.org/10.1016/j.virs.2022.06.003.

References

An, T.Q., Peng, J.M., Tian, Z.J., Zhao, H.Y., Li, N., Liu, Y.M., Chen, J.Z., Leng, C.L., Sun, Y., Chang, D., Tong, G.Z., 2013. Pseudorabies virus variant in Bartha-K61-vaccinated pigs, China, 2012. Emerg Infect Dis 19, 1749–1755.

Ashburner, M., Ball, C.A., Blake, J.A., Botstein, D., Butler, H., Cherry, J.M., Davis, A.P., Dolinski, K., Dwight, S.S., Eppig, J.T., 2000. Gene ontology: tool for the unification of biology. Nat. Genet. 25, 25.

Beausoleil, S.A., Villén, J., Gerber, S.A., Rush, J., Gygi, S.P., 2006. A probability-based approach for high-throughput protein phosphorylation analysis and site localization. Nature biotechnology 24, 1285.

Beck, F., Geiger, J., Gambaryan, S., Solari, F.A., Dell'Aica, M., Loroch, S., Mattheij, N.J., Mindukshev, I., Pötz, O., Jurk, K., Burkhart, J.M., Fufezan, C., Heemskerk, J.W., Walter, U., Zahedi, R.P., Sickmann, A., 2017. Temporal quantitative phosphoproteomics of ADP stimulation reveals novel central nodes in platelet activation and inhibition. Blood 129, e1–e12.
Bhoumik, A., Ronai, Z., 2008. ATF2-A transcription factor that elicits oncogenic or tumor suppressor activities. Cell Cycle 7, 2341–2345.
Duzgun, S.A., Yerlikaya, A., Zeren, S., Bayhan, Z., Okur, E., Boyaci, I., 2017. Differential effects of p38 MAP kinase inhibitors SB203580 and SB202190 on growth and migration of human MDA-MB-231 cancer cell line. Cytotechnology 69, 711–724.
Flori, L., Rogel-Gaillard, C., Cochet, M., Lemonnier, G., Hugot, K., Chardon, P., Robin, S., Lefevre, F., 2008. Transcriptomic analysis of the dialogue between Pseudorabies virus and porcine epithelial cells during infection. BMC Genom. 9, 123.
Freuling, C.M., Muller, T.F., Mettenleiter, T.C., 2017. Vaccines against pseudorabies virus (PrV). Vet. Microbiol. 206, 3–9.
Gueorguiev, V.D., Cheng, S.Y., Sabban, E.L., 2006. Prolonged activation of cAMP-response element-binding protein and ATF-2 needed for nicotine-triggered elevation of tyrosine hydroxylase gene transcription in PC12 cells. J. Biol. Chem. 281, 10188–10195.
Gupta, S., Campbell, D., Derijard, B., Davis, R.J., 1995. Transcription factor ATF2 regulation by the JNK signal transduction pathway. Science 267, 389–393.
Hai, T.W., Liu, F., Coukos, W.J., Green, M.R., 1989. Transcription factor ATF cDNA clones: an extensive family of leucine zipper proteins able to selectively form DNA-binding heterodimers. Genes Dev. 3, 2083–2090.
He, F., Xiao, Z., Yao, H., Li, S., Feng, M., Wang, W., Liu, Z., Wu, J., 2019. The protective role of microrna-21 against coxsackievirus b3 infection through targeting the map2k3/p38 mapk signaling pathway. J. Transl. Med. 17, 335.
Inoue, S., Mizushima, T., Ide, H., Jiang, G., Goto, T., Nagata, Y., Netto, G.J., Miyamoto, H., 2018. ATF2 promotes urothelial cancer outgrowth via cooperation with androgen receptor signaling. Endocr. Connect 7, 1397–1408.
Kanehisa, M., Goto, S., 2000. KEGG: Kyoto encyclopedia of genes and genomes. Nucleic Acids Res. 28, 27–30.
Kumar, A., Manna, S.K., Dhawan, S., Aggarwal, B.B., 1998. HIV-tat protein activates c-Jun N-terminal kinase and activator protein-1. J. Immunol. 161, 776–781.
Larsen, M.R., Thingholm, T.E., Jensen, O.N., Roepstorff, P., Jørgensen, T.J.D., 2005. Highly selective enrichment of phosphorylated peptides from peptide mixtures using Titanium dioxide microcolumns. Mol. Cell. Proteomics 4, 873–886.
Li, A., Lu, G., Qi, J., Wu, L., Tian, K., Luo, T., Shi, Y., Yan, J., Gao, G.F., 2017. Structural basis of nectin-1 recognition by pseudorabies virus glycoprotein D. PLoS Pathog. 13, e1006314.
Lim, J.Y., Park, S.J., Hwang, H.Y., Park, E.J., Nam, J.H., Kim, J., Park, S.I., 2005. TGF-beta 1 induces cardiac hypertrophic responses via PKC-dependent ATF-2 activation. J. Mol. Cell. Cardiol. 39, 627–636.
Liu, F., Zheng, H., Tong, W., Li, G.X., Tian, Q., Liang, C., Li, L.W., Zheng, X.C., Tong, G.Z., 2016. Identification and analysis of novel viral and host dysregulated micrornas in variant pseudorabies virus-infected pk15 cells. PLoS One 11, e0151546.
Ma, J., Chang, K., Peng, J., Shi, Q., Gan, H., Gao, K., Feng, K., Xu, F., Zhang, H., Dai, B., Zhu, Y., Shi, G., Shen, Y., Zhu, Y., Qin, X., Li, Y., Zhang, P., Ye, D., Wang, C., 2018. Spop promotes atf2 ubiquitination and degradation to suppress prostate cancer progression. J. Exp. Clin. Cancer Res. 37, 145.
Macek, B., Mann, M., Olsen, J.V., 2009. Global and site-specific quantitative phosphoproteomics: principles and applications. Annu. Rev. Pharmacol. Toxicol. 49, 199–221.
McLean, T., Bachenheimer, S., 1999. Activation of cjun n-terminal kinase by herpes simplex virus type 1 enhances viral replication. J. Virol. 73, 8415–8426.
Mettenleiter, T.C., 2000. Aujeszky's disease (pseudorabies) virus: the virus and molecular pathogenesis-state of the art. Vet. Res. 31, 99–115.
Mosmann, T., 1983. Rapid colorimetric assay for cellular growth and survival: application to proliferation and cytotoxicity assays. J. Immunol. Methods 65, 55–63.
Moynagh, J., 1997. Aujeszky's disease and the European Community. Vet. Microbiol. 55, 159–166.
Murata, T., Noda, C., Saito, S., Kawashima, D., Sugimoto, A., Isomura, H., Kanda, T., Yokoyama, K.K., Tsurumi, T., 2011. Involvement of jun dimerization protein 2 (jdp2) in the maintenance of epstein-barr virus latency. J. Bio. Chem. 286, 22007–22016.
Olsen, J.V., Blagoev, B., Gnad, F., Macek, B., Kumar, C., Mortensen, P., Mann, M., 2006. Global, in vivo, and site-specific phosphorylation dynamics in signaling networks. Cell 127, 635–648.
Ouwens, D.M., de Ruiter, N.D., van der Zon, G.C., Carter, A.P., Schouten, J., van der Burgt, C., Kooistra, K., Bos, J.L., Maassen, J.A., van Dam, H., 2002. Growth factors can activate ATF2 via a two-step mechanism: phosphorylation of Thr71 through the Ras-MEK-ERK pathway and of Thr69 through RalGDS-Src-p38. Embo J. 21, 3782–3793.
Pensaert, M., Morrison, R., 2000. Challenges of the final stages of the adv eradication program. Vet. Res. 31, 141–145.
Ravikumar, V., Jers, C., Mijakovic, I., 2015. Elucidating host-pathogen interactions based on post-translational mmodifications using proteomics aapproaches. Front. Microbiol. 6, 1313.
Söderholm, S., Kainov, D.E., Öhman, T., Denisova, O.V., Schepens, B., Kulesskiy, E., Imanishi, S.Y., Corthals, G., Hintsanen, P., Aittokallio, T., 2016. Phosphoproteomics to characterize host response during influenza A virus infection of human macrophages. Mol. Cell. Proteomics 15, 3203–3219.
Recio, J.A., Merlino, G., 2002. Hepatocyte growth factor/scatter factor activates proliferation in melanoma cells through p38 MAPK, ATF-2 and cyclin D1. Oncogene 21, 1000–1008.
Rodems, S.M., Spector, D.H., 1998. Extracellular signal-regulated kinase activity is sustained early during human cytomegalovirus infection. J. Virol. 72, 9173–9180.
Salinas-Abarca, A.B., Velazquez-Lagunas, I., Franco-Enzástiga, Ú., Torres-López, J.E., Rocha-González, H.I., Granados-Soto, V., 2018. ATF2, but not ATF3, participates in the maintenance of nerve injury-induced tactile allodynia and thermal hyperalgesia. Mol. Pain 9, 12.
Schagger, H., 2006. Tricine-SDS-PAGE. Nat. Protocols 1, 16–22.
Sharma-Walia, N., Krishnan, H.H., Naranatt, P.P., Zeng, L., Smith, M.S., Chandran, B., 2005. ERK1/2 and mek1/2 induced by kaposi's sarcoma-associated herpesvirus (human herpesvirus 8) early during infection of target cells are essential for expression of viral genes and for establishment of infection. J. Virol. 79, 10308–10329.
Shen, H., Wu, N., Wang, Y., Han, X., Zheng, Q., Cai, X., Zhang, H., Zhao, M., 2017. JNK inhibitor SP600125 aparaquat-induced alung injury: an in vivo and in vitro study. Inflammation 40, 1319–1330.
Stevens, J.G., Wagner, E., Devi-Rao, G., Cook, M., Feldman, L., 1987. RNA complementary to a herpesvirus alpha gene mRNA is prominent in latently infected neurons. Science 235, 1056–1059.
Tombacz, D., Toth, J.S., Boldogkoi, Z., 2011. Deletion of the virion host shut: off gene of pseudorabies virus results in selective upregulation of the expression of early viral genes in the late stage of infection. Genomics 98, 15–25.
van Dam, H., Wilhelm, D., Herr, I., Steffen, A., Herrlich, P., Angel, P., 1995. ATF-2 is preferentially activated by stress-activated protein kinases to mediate c-jun induction in response to genotoxic agents. EMBO J. 14, 1798–1811.
Wang, L., Payton, R., Dai, W., Lu, L., 2011. Hyperosmotic Stress-induced ATF-2 Activation through Polo-like Kinase 3 in Human Corneal Epithelial Cells. J. Biol. Chem. 286, 1951–1958.
Wang, X., Wu, C.-X., Song, X.-R., Chen, H.-C., Liu, Z.-F., 2017. Comparison of pseudorabies virus China reference strain with emerging variants reveals independent virus evolution within specific geographic regions. Virology 506, 92–98.
Wang, X., Zhang, M.-M., Yan, K., Tang, Q., Wu, Y.-Q., He, W.-B., Chen, H.-C., Liu, Z.-F., 2018. The full-length microRNA cluster in the intron of large latency transcript is associated with the virulence of pseudorabies virus. Virology 520, 59–66.
Wojcechowskyj, J.A., Didigu, C.A., Lee, J.Y., Parrish, N.F., Sinha, R., Hahn, B.H., Bushman, F.D., Jensen, S.T., Seeholzer, S.H., Doms, R.W., 2013. Quantitative phosphoproteomics reveals extensive cellular reprogramming during HIV-1 entry. Cell Host Microbe 13, 613–623.
Wu, Y.Q., Chen, D.J., He, H.B., Chen, D.S., Chen, L.L., Chen, H.C., Liu, Z.F., 2012. Pseudorabies virus infected porcine epithelial cell line generates a diverse set of host microRNAs and a special cluster of viral microRNAs. PLoS One 7, e30988.
Xie, S., Shen, B., Zhang, C., Huang, X., Zhang, Y., 2014. sgRNAcas9: a software package for designing CRISPR sgRNA and evaluating potential off-target cleavage sites. PLoS One 9, e100448.
Xing, J., Liang, J., Liu, S., Huang, L., Hu, P., Liu, L., Liao, M., Qi, W., 2021. Japanese encephalitis virus restricts hmgb1 expression to maintain mapk pathway activation for viral replication. Vet. Microbiol. 262, 109237.
Yan, K., Liu, J., Guan, X., Yin, Y.-X., Peng, H., Chen, H.-C., Liu, Z.-F., 2019. The ctterminus of ttegument protein pUL 21 contributes to pseudorabies virus neuroinvasion. J. Virol. 93 e02052-2018.
Yang, S., Pei, Y., Zhao, A., 2017. iTRAQ-based proteomic analysis of porcine kidney epithelial PK15 cells infected with pseudorabies virus. Sci. Rep. 7, 45922.
Yeh, C.J., Lin, P.Y., Liao, M.H., Liu, H.J., Lee, J.W., Chiu, S.J., Hsu, H.Y., Shih, W.L., 2008. TNF-alpha mediates pseudorabies virus-induced apoptosis via the activation of p38 MAPK and JNK/SAPK signaling. Virology 381, 55–66.
Yin, Y., Romero, N., Favoreel, H.W., 2021. Pseudorabies virus inhibits type I and type III interferon-induced signaling via proteasomal degradation of janus kinases. J. Virol. 95, e0079321.
Yu, X.L., Zhou, Z., Hu, D., Zhang, Q., Han, T., Li, X., Gu, X., Yuan, L., Zhang, S., Wang, B., 2014. Pathogenic pseudorabies virus, china, 2012. Emerg. Infect. Dis. 20, 102–104.
Yuan, Z., Gong, S., Luo, J., Zheng, Z., Song, B., Ma, S., Guo, J., Hu, C., Thiel, G., Vinson, C., Hu, C.D., Wang, Y., Li, M., 2009. Opposing roles for ATF2 and c-Fos in c-Jun-mediated neuronal apoptosis. Mol. Cell Biol. 29, 2431–2442.
Yuan, J, Liu, X., Wu, A.W., McGonagill, P.W., Keller, M.J., Galle, C.S., Meier, J.L., 2009. Breaking human cytomegalovirus major immediate-early gene silence by vasoactive intestinal peptide stimulation of the protein kinase a-creb-torc2 signaling cascade in human pluripotent embryonal ntera2 cells. J. Virol. 83, 6391–6403.
Zachos, G., Clements, B., Conner, J., 1999. Herpes simplex virus type 1 infection stimulates p38/c-Jun N-terminal mitogen-activated protein kinase pathways and activates transcription factor AP-1. J. Biol. Chem. 274, 5097–5103.
Zhu, Z.X., Li, W.W., Zhang, X.L., Wang, C.C., Gao, L.L., Yang, F., Cao, W.J., Li, K.L., Tian, H., Liu, X.T., Zhang, K.S., Zheng, H.X., 2020. Foot-and-mouth disease virus capsid protein vp1 interacts with host ribosomal protein sa to maintain activation of the mapk signal pathway and promote virus replication. J. Virol. 94, e01350-19.